
Modeling of Load-Bearing Behavior of Fiber-Reinforced Concrete Tunnel Linings

By Axel G. Nitschke

The use of fiber-reinforced concrete (FRC)—with steel or macro-synthetic fibers—has technical and economic advantages that primarily stem from the fact that fibers transform the post-cracking behavior from a brittle failure mode typical of unreinforced concrete into an elasto-plastic behavior. Numerous codes and guidelines provide qualitative or quantitative design approaches.¹⁻⁶ Modeling of the load-bearing behavior based on a stress-strain relationship (SSR) for tunneling applications is commonly used. This article discusses the modeling process and some typical results of a parameter study. It also identifies the weakness of the current concept and suggests a path to more fully use the structural and economic potential of FRC. The concept discussed herein is theoretical in nature and applicable for both steel and synthetic FRC. To limit the scope of this article, the discussion is focused on the load-bearing capacity under cracked conditions, which is typical for shotcrete initial linings. Therefore, design concepts that do not use the toughness potential of FRC (that is, by limiting it to uncracked conditions) are not discussed herein.

Different international codes and guidelines for FRC provide testing procedures based on simply supported beam tests that are used to define an SSR by basically amending the known trapezoidal or parabolic SSR for concrete on the compression side with assumptions for an SSR on the tension side. The latter is the primary subject of this article. For this discussion, it is irrelevant which type of macrofibers—steel or synthetic—is used because the SSR models a homogeneous, composite material behavior and not discrete fibers. In general, the SSR design approach follows the concept to adapt existing concrete design concepts and procedures and simply extend the SSR on the tension side to account for the effect of the properties of the composite material.

This article is focused solely on combined moment thrust or moment normal force (M/N) loading of tunnel linings in which bearing capacity relies on a tunnel arch. This is typical for soft ground tunnel linings and rock tunnels with soft-ground-like behavior. Nonetheless, the ideas and concepts can also be adapted in typical rock tunneling applications. However, they are not useful in tunnels with no arching effect, which is typical for tunnels

with relatively thin linings or with an irregular shape. For these types of tunnels (that is, typical initial linings in classical rock tunneling), qualitative and empirical design concepts (for example, Barton chart^{7,8}) are available but are not discussed in this paper.

The use of an SSR is typically evaluated on the basis of beam test data. Under elastic (uncracked) conditions, the beam theory and the classical mechanics for materials apply. However, after the initial cracking of the FRC, the material is no longer homogeneous and the theoretical conditions for beam theory no longer apply. The bearing behavior of FRC in beam tests in a cracked state are better described using a stress-crack width relationship rather than a stress-strain relationship. It is important to understand that for the aforementioned reason, an SSR cannot be measured directly in standard FRC beam tests. The codes and guidelines are therefore describing testing procedures that measure external forces and deformations, which are then transformed into stresses and “equivalent” strains via an equivalence model, which implies several assumptions. Research by Nitschke⁹ has discussed flaws in some of these models by back-calculation of tests using the SSRs. It was shown that these flaws can be significant under loading conditions of combined moment and thrust, typical for tunneling. The same work also provided modified models to provide more useable and accurate procedures.⁹

STRUCTURAL BASICS OF FRC DESIGN

The biggest difference between the sectional strength of unreinforced or steel bar reinforced concrete and FRC is that the concrete in unreinforced or bar-reinforced concrete has (theoretically) no bearing capacity in tension. In the modeling of conventionally reinforced concrete sections, all tension is supported by the reinforcing bar. Because the location of the reinforcing bar is known, the location of the resulting tensile force is also known, and this simplifies the calculation of the equilibrium compared to FRC sections. The computation of axial equilibrium in FRC sections is much more challenging because the location of the resulting tensile force is an unknown during the computation and moves if the external load and the distribution of the strain over the cross section changes.

The design assumptions for the calculation of the sectional strength for FRC based on an SSR can be summarized as follows¹⁰ (ACI 318-14, Section 22.2,¹¹ ACI Design Handbook, Section 7.4¹²):

1. Equilibrium shall be satisfied at each section;
2. Strain in the cross section of the member shall be assumed directly proportional to the distance from the neutral axis (Bernoulli's theorem). The cross section also remains plane during loading;
3. The stress-strain relationship for the FRC in compression is defined; thus, the stress for a given strain is known within defined limits; and
4. The stress-strain relationship of the FRC under tension is defined; thus, the stress for a given strain is known within defined limits.

A comparison of the essential design assumptions for moment and axial strength at sections for reinforcing bar reinforced concrete design in ACI 318 shows that the first and second assumptions—equilibrium (ACI 318-14, Section 22.2.1.1¹¹) and Bernoulli (ACI 318-14, Section 22.2.1.2¹¹)—are adapted for FRC. However, by citing two additional design assumptions from ACI 318, two major differences between FRC and classical bar reinforced designs assumptions can also be highlighted. According to ACI 318-14, Section 22.2.2.2¹¹:

“Tensile strength of concrete shall be neglected in flexural and axial strength calculations.”

For sectional strength calculation of FRC, the tensile strength under uncracked as well as cracked conditions is used. This is one of the major differences between the modeling of FRC in comparison with unreinforced or bar-reinforced concrete.

According to ACI 318-14, 22.2.1.2¹¹:

“Strain in concrete and non-prestressed reinforcement shall be assumed proportional to the distance from the neutral axis.”

This design assumption is based on the hypothesis of perfect bonding between steel and concrete. While bar-reinforced concrete is modeled as a composite of concrete and steel, where each component has its own material properties (refer to ACI 318-14, Section 22.2.2, for concrete and Section 22.2.3 for non-prestressed reinforcement¹¹), FRC is assumed to be a macroscopically homogeneous and isotropic material.¹³ The material properties of a single fiber in the model becomes irrelevant. Therefore, the fibers and the concrete are modeled using a single SSR relationship and not two (that is, as for steel reinforcing bar and concrete).

After the cracking of the FRC material under tension, the material properties in the model are based on strains rather than a discrete crack. In the model, the cracked material is also viewed as homogeneous and isotropic. Because this is in the area around the crack, it is obviously not the case. This circumstance is very important to realize and understand when evaluating the sectional strength of FRC using an SSR. During the evaluation of material testing data based on beam tests (and subsequently the design of the structure), it is assumed that the crack is “smeared” over a cer-

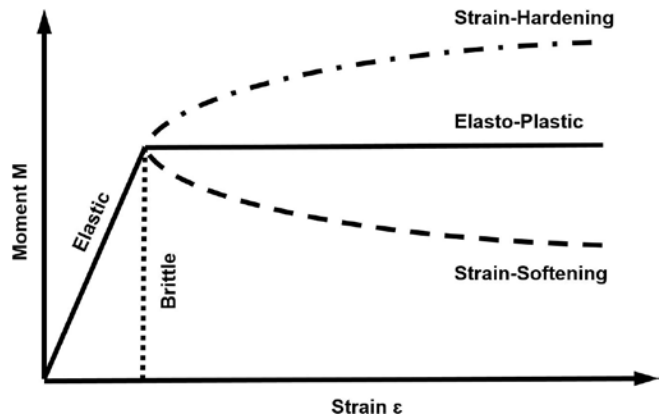


Fig. 1: Schematic post-peak response of fiber-reinforced concrete

tain length into an “equivalent strain,” which is also referred to as the “integral approach.”¹⁰

Fibers influence the bearing behavior in multiple ways. However, three properties are most relevant for application in tunnels.¹³ They slightly increase the flexural tensile strength (1), which is mostly needed if improved properties under uncracked conditions are desired (that is, to design for serviceability.) However, for the case of ultimate bearing capacity of tunnel linings, the residual flexural tensile strength under cracked conditions (2) and the increase of the toughness (3) are the major benefits. The focus of this paper is on the performance improvements attributable to (2) and (3).

The provision of a reliable and usable post-cracking tensile strength transforms the brittle failure mechanism of plain concrete into a ductile failure mode (refer to Fig. 1). This is a material property that provides major engineering and economic advantages, especially if used to facilitate system failure of a tunnel lining rather than a cross section failure at one presumably most-critical location. A concept for the design of a system failure will be presented later in this article.

According to Dietrich,¹⁰ the load-bearing response of FRC under bending can be subdivided into three phases. The first “uncracked” phase is based on the behavior of the concrete matrix alone. The concrete matrix and fibers are assumed to be in “perfect bond” and the ratio of load supported by the concrete compared to the fibers is dependent on the moduli of elasticity of the materials. Due to the relatively small volume of fibers compared to concrete, the load-bearing share of the fibers is relatively small.

Microcracks develop in the matrix during the second phase of load response. The development of cracks is hampered by the fibers and leads, according to Dietrich,¹⁰ to a more stable “strain softening” with a restricted expansion of cracks and less brittle material behavior. Phase two ends with crack widths of approximately 0.004 in. (0.1 mm).¹⁰

In the third phase, the concrete matrix no longer provides significant bearing capacity at the crack. The opening cracks are bridged by the fibers and the load transfer is effectively provided by the fibers alone.

SECTION DESIGN OF FRC USING STRESS-STRAIN RELATIONSHIP

The three phases of crack development are also reflected in SSRs found in different codes and guidelines. Studies by Nitschke^{9,15} have shown that by using all three phases in computer simulations, test results obtained using beam tests can be simulated very accurately. Typically, all SSRs in codes and guidelines incorporate Phase I (elastic) and Phase III (macrocrack) behavior. However, because the distinction between uncracked and microcracking in Phase II is not clearly defined, Phase I and Phase II are oftentimes lumped together or Phase II is completely neglected.⁹ It is important to note that for the modeling of ultimate load-bearing capacity in the macrocracked phase, a detailed evaluation of the microcracking Phase II is irrelevant. However, it might be significant for serviceability design.

A generic SSR and nomenclature of the variables used throughout this paper is shown in Fig. 2. The tension side is represented by the three sections discussed previously. The compression side uses a classical parabolic constant shape.

Nitschke⁹ has conducted numerous simulations of beam test results under pure bending as well as combined M/N loading. The three load-bearing phases observed during the experimental studies could also be reflected with the simulation of the load-bearing behavior, using the SSR as follows. In general, it is possible to identify “typical” SSRs based on typical load-deflection curves from either tests or the simulation of results. By adhering to certain boundary conditions, it is almost possible to look at each of the three phases separately.⁹

The pure elastic (uncracked) behavior is related to the first part of the stress-strain relationship and conforms to the principles of elastic bending. The flexural strength f_{t1} results from the maximum elastic moment divided by the section modulus. The range of the related strain ϵ_{t1} is very limited and can either be measured during the test or—based on the used SSR—be calculated using the original modulus of elasticity. Alternatively, and if the major focus of the interest is the bearing capacity under cracked condi-

tions, a generic value between $0.1\% \leq \epsilon_{t1} \leq 0.15\%$ (100 to 150 microstrain) will yield sufficiently accurate results because the overall influence of the elastic section on the bearing capacity under cracked conditions is diminished.⁹

The interim section of microcracking is reflected by the second section of the SSR on the tension side. In general, two different types of curves are used between ϵ_{t1} and ϵ_{t2} : 1) a plateau; or 2) a linearly decreasing curve (trapezoid). By using a plateau, the stress in the second section is constant ($f_{t2a} = f_{t1}$) (refer to Fig. 2). In general, the plateau creates load-deflection curves with a distinct maximum and a “hard” decline of the moment-bearing capacity in pure bending conditions. On the other hand, a declining curve in the second section ($f_{t2a} \geq f_{t2b}$) (refer to Fig. 2) “softens” this area of the moment-deflection curve.⁹

More complex curves can be used in the second section; however, the two selected types may encompass many other cases. As parameter studies have shown,⁹ the overall influence of the second section of the SSR controls the shape of a specific area of the simulation of the bearing capacity but has only a small influence on the overall bearing capacity. It was also shown that more important than the value of the stress f_{t2b} is the specific strain ϵ_{t2} , which controls the shape of a moment-deflection curve in this area.⁹

However, by far the biggest influence on the load-bearing behavior under cracked conditions is the third section of the SSR. The tensile stress under cracked conditions is typically referred to as the “residual strength.” Under consideration of the conducted beam tests with a maximum deflection of 0.14 in. (3.5 mm), SSRs up to a strain of $\epsilon_{t3} = 25\%$ were investigated.

The load-bearing capacity of a cross section based on the SSR is calculated by finding the equilibrium between internal and external forces. Only a discussion of the basic principle is covered in this paper. A complete solution for the calculation of the inner forces resulting from a specific strain scenario is provided by Nitschke.⁹ For the calculation of equilibrium between internal and external forces acting on

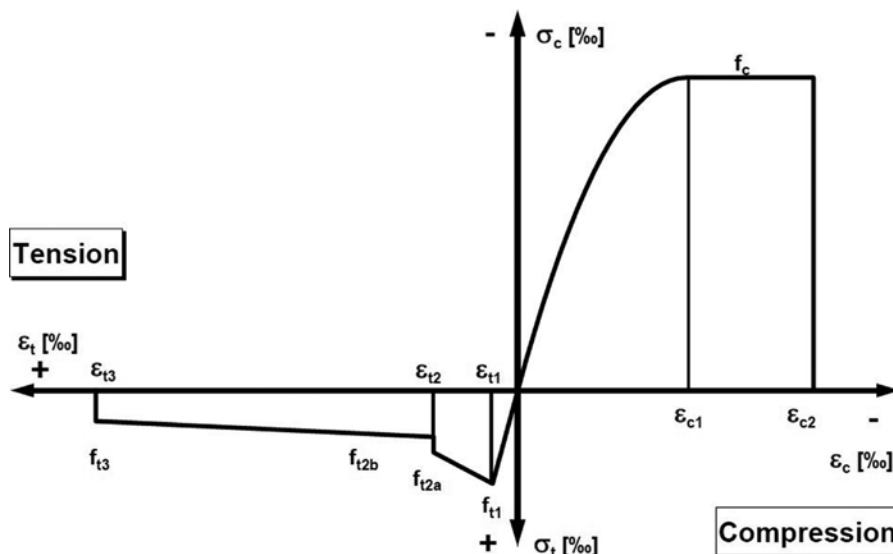


Fig. 2: Generic stress-strain relationship for fiber-reinforced concrete

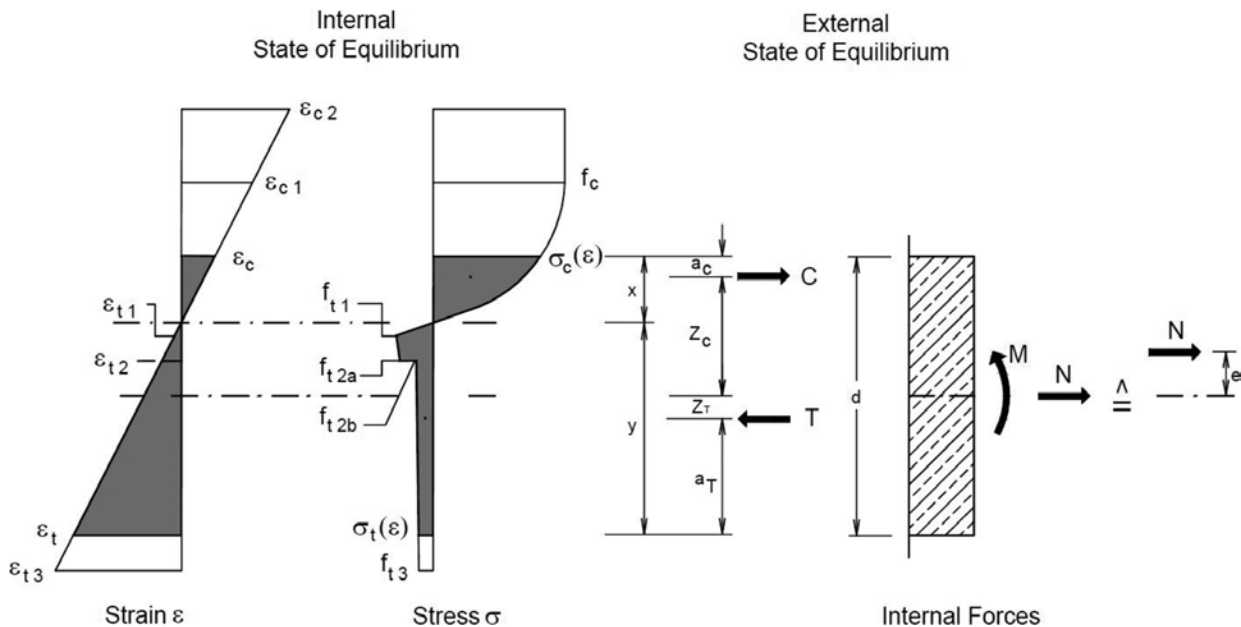


Fig. 3: Calculation of equilibrium between internal and external forces

a cross section under typical tunneling conditions, there are two equations (refer to Fig. 3)

$$\begin{aligned} \sum N = 0 &\Leftrightarrow C - T + N = 0 \\ \sum M = 0 &\Leftrightarrow -C \cdot z_c - T \cdot z_T + M = 0 \end{aligned}$$

The internal lever arm z , as well as the height of the compression zone x and height of the tension zone y are calculated as follows

$$\begin{aligned} z_c &= \frac{d}{2} - a_c & z_T &= \frac{d}{2} - a_T \\ x &= \frac{|\epsilon_c|}{|\epsilon_c| + |\epsilon_t|} d & y &= \frac{|\epsilon_t|}{|\epsilon_c| + |\epsilon_t|} d \end{aligned}$$

for $\epsilon_c \leq 0$ and $\epsilon_t \geq 0$

Because only two equations for the equilibrium are available, all but two variables must be known to compute a unique solution. However, at first there are four unknowns: the resulting thrust (C), the resulting tensile force (T), and their respective levers (z_c, z_T). All four unknowns are directly related to the existing strain condition. By selecting a specific strain condition, the moment capacity, as well as the normal force capacity, can be calculated and the result is unique.

Theoretically, the reversed approach—selection of the external forces followed by the calculation of the corresponding strain condition—is possible. However, this solution is practically not achievable because, typically, an SSR of FRC is discontinuous and depends on numerous parameters. In addition, the solution often provides multiple equilibriums and is therefore not unique.⁹ As a result, an iterative process is necessary to solve the equations, which requires a lot of computation effort.¹⁴

LOAD-BEARING BEHAVIOR AND DESIGN OF FRC UNDER COMBINED m/n LOADING

Moment-normal force interaction diagrams (MNID) are typically used during the design of tunnel linings (and columns under combined M/N loading in general) for steel bar reinforced linings as well as FRC. However, while generic MNID are available for bar-reinforced members, an SSR-specific MNID has to be developed for FRC. Generic MNIDs for FRC can be developed in a similar fashion to bar-reinforced members if the diagrams are dimensionless and all strength values are defined (that is, relative to the compressive strength f_c .) The dimensionless factor $n = N/(f_c \times b \times d)$ can hereby be interpreted as the use toward the maximum thrust under pure compression. The SSR used for the following parameter studies is defined in Table 1 and represents

Table 1: Stress-Strain Relationship used in the Parameter Study

Stress	Tension				Compression	
	f_{t3}	f_{t2b}	f_{t2a}	f_{t1}	f_{c1}	f_{c2}
N/mm ²	0.5	1.0	4.0	4.0	-40.0	-40.0
% of f_c	1.25	2.5	10	10	100	100
Strain	ϵ_{t3}	ϵ_{t2b}	ϵ_{t2a}	ϵ_{t1}	ϵ_{c1}	ϵ_{c2}
‰	10.0	0.16	0.16	0.12	-2.0	-3.5

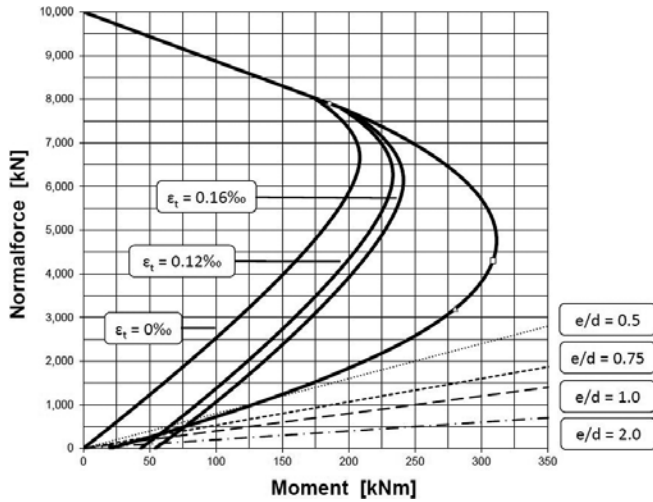


Fig. 4: Moment normal force interaction diagram (MNID)

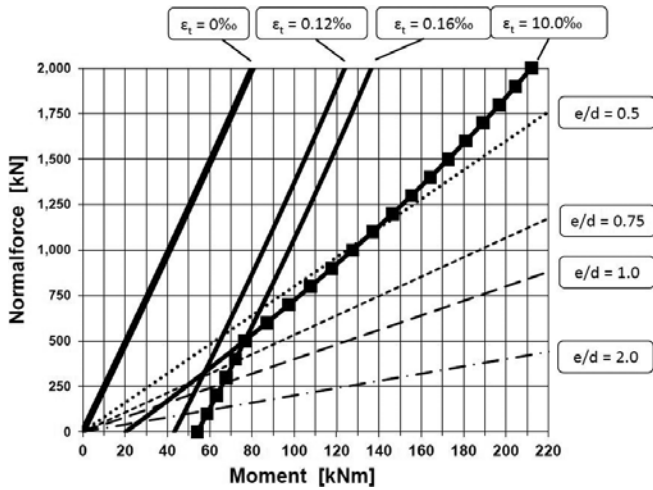


Fig. 5: MNID—enlarged section relevant for tunneling

typical values for FRC (that is, an initial tunnel lining.) For the nomenclature and shape, refer to the SSR in Fig. 2. The thickness of the lining was assumed to be 10 in. (0.25 m) and a 3.2 ft (1.0 m) wide tunnel lining section was assumed.

Figure 4 shows the complete MNID for the SSR presently used, while Fig. 5 shows an enlarged section of the same MNID. Focus on investigations are typically lines with a constant normal force, parallel to the x-axis, or lines with a constant “e/d ratio,” which are inclined and intersecting the origin of the MNID. The dimensionless e/d ratio is defined as the eccentricity e over beam height d, with $e = M/N$. Figure 6 shows the results of a parameter study with varying e/d ratios; Fig. 7 shows a parameter study for varying normal forces.

It is important to highlight that all figures are basically different ways of displaying the bearing capacity of the same material, defined in Table 1. The results represented—for example, along the e/d = 0.5 line in Fig. 5—are the same as shown in Fig. 6 for the identical case. The results represented in Fig. 5 on a line with a constant normal force, parallel to the x-axis—that is, $N = 1000$ kN—is the same as shown in Fig. 7

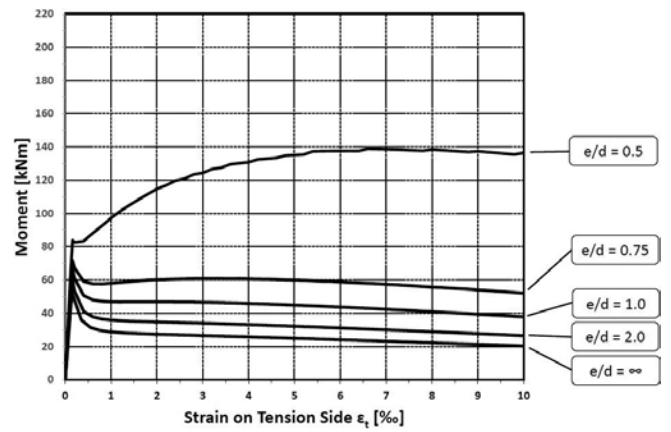


Fig. 6: Moment-strain diagram, parameter study e/d ratio

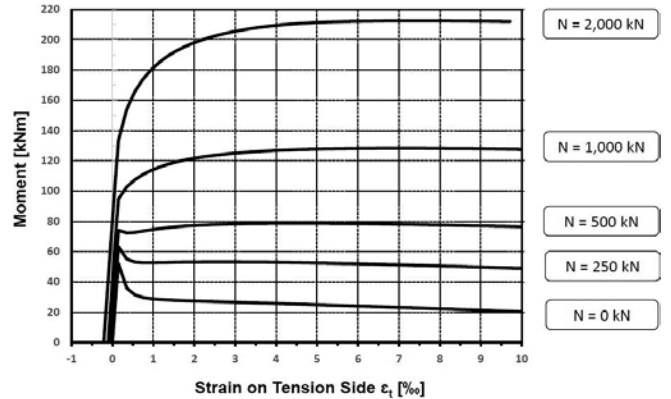


Fig. 7: Moment-strain diagram, parameter study normal force

for the same thrust. The bearing behavior under pure bending ($N = 0$; $e/d = \infty$) is represented on the x-axis in the MNID.

The example shown could also be transferred into a generic dimensionless MNID by using the following equations for the normal force and the moment

$$n = \frac{N}{f_c \times b \times d} \quad m = \frac{M}{f_c \times b \times d^2}$$

The residual strength f_{t1} on the tension side can be expressed as a percentage of the compressive strength (refer to Table 1). The dimensionless MNID would be valid for all cases where the ratios between the tensile strength and the compressive strength are kept the same. The different lines in the MNID show cross section equilibriums for specific constant tension strains.

A good rule of thumb is that tunnel linings are typically using between 5 and 30% of the compression capacity of a member.⁹ So, for example, in the MNID in Fig. 4, a typical use in a soft ground tunnel would be between 0.5 and 3 MN and only the lower one-third of the diagram would be relevant for the design; Fig. 5 shows this area of the MNID enlarged. Tunnel linings in this part of an MNID generally fail under tension by reaching the maximum allowable tensile strain ϵ_{t3} .

The different lines in the MNIDs represent lines of specific strains (Fig. 4 and 5). Left of the line marked with $\epsilon_t = 0\%$ –

tensile strain zero – all members are under full compression. The $\epsilon_t = 0.12\%$ respectively $\epsilon_t = 0.16\%$ -lines represent the end of the elastic behavior (Phase I/II) respectively the beginning of macro-cracking (Phase II/III). The $\epsilon_t = 10.0\%$ line represents equilibriums reaching the maximum tensile strain defined for this example. Following this line into the area between $N = 0$ kN and $N = 500$ kN (Fig. 5) shows the area of pure bending in which axial thrust has a very small influence. In this area, the bearing capacity in the elastic state ($\epsilon_t = 0.12\%$) and the microcracked state ($\epsilon_t = 0.16\%$) is larger than the load in the cracked phase ($0.16\% < \epsilon_t \leq 10.0\%$). That means the ultimate load is less than the peak load reached around the elastic/uncracked state (also refer to Fig. 6, $e/d = \infty, 2.0, 1, 0$, and 0.75 and Fig. 7, $N = 0, 250, 500$ kN). This shows the typical strain-softening behavior of FRC in bending tests (refer to Fig. 1). The intersection of the $\epsilon_t = 0.16\%$ – line and the $\epsilon_t = 10\%$ – line in the MNID marks the point of quasi ideal elasto-plastic behavior, meaning the maximum load level reached under uncracked or microcracked conditions can be maintained, which is reached in this example at roughly $N = 500$ kN (Fig. 1, 5, and 7).

The simulated examples, which are representative of behavior observed in tests, also show that the moment-bearing capacity in the elastic, the microcracking, and the cracked phase are all increased under the influence of an increasing normal compressive force. While typical FRC simply supported bending tests show a strain-softening behavior, it can be observed that an increased normal force leads to a quasi elasto-plastic and a quasi strain-hardening effect. The term “quasi” is used because the bending behavior is a characteristic of the structural system; material properties do not actually change. For the same material, the bearing behavior changes with an increased normal force influence (Fig. 1, 5, 6, and 7).

Figure 1 shows the difference between elastic-brittle, elasto-plastic, and strain-hardening behavior, and strain softening in a simplified manner. Strain-softening behavior is typical for pure bending; the moment-bearing capacity decreases after the peak load. An increased normal force influence leads to nearly elasto-plastic system performance (in our example for $N \approx 500$ kN [refer to Fig. 7] and $0.5 < e/d < 0.75$ [refer to Fig. 6], respectively) and under a further increased normal force influence, the behavior progresses to a quasi strain-hardening effect. In addition to a change in failure mode, represented by the shape of the curve, there is also an increase in the peak moment capacity. While in the example the maximum bearable moment at 10% tensile strain is around 20 kNm, every 100 kN additional normal force increases the moment-bearing capacity by roughly 10 kNm in this example.

FRC SPECIFICATION BASED ON RANGE OF NORMAL FORCE

What do these results mean for a tunnel lining design and FRC specification? The general desire from a structural perspective for a tunnel lining design under cracked conditions requires that the bearing capacity under

cracked conditions shall be equal to or higher than the bearing capacity in the elastic state. Referring to Fig. 1, the behavior shall be at least “elasto-plastic” or display “strain hardening.” In the previous section, it was shown that these conditions are highly dependent on the amount of normal force in the system. However, current tunnel designs do not take the range of expected normal force into consideration when specifying the material properties of FRC. Therefore, a lot of structural potential of FRC remains underused.

If elasto-plastic behavior or strain-hardening behavior is desired, material specifications should take the expected range of normal force, represented by the mean compressive stress in the lining, into consideration. The range of expected normal force, respectively the compressive strength in a lining, can be easily evaluated based on preliminary lining designs. As shown in the parameter study herein, a project-specific SSR could be specified that meets or exceeds the requirements. Subsequently, pure bending or tests under combined moment-normal force could be used to prove that the SSR requirements could be met. Rather than the absolute values for the residual strength, it is suggested to specify an SSR with strength values relative to the compressive strength of the material.

INELASTIC STRUCTURAL ANALYSIS USING PLASTIC HINGES

ACI 318 and other international codes provide several options for a structural analysis of reinforced concrete structures. In a typical tunnel design the forces of the lining are determined in a linear-elastic model. Representative pairs of moments and normal forces from this analysis are then transferred into a MNID to ensure that the load combinations can be born by the FRC lining.

As discussed previously, the inclusion of fibers increases the moment-bearing capacity compared to unreinforced concrete when a section is subject to a large compressive normal force. However, typically even light steel bar reinforcement can do the same or even exceed the bearing capacity of FRC. Where, then, is the benefit of FRC in the structural design? The benefit of FRC lies in the added toughness of the material, which allows—under elasto-plastic or strain-hardening conditions—to “hold” a moment in a lining even under severe deformation of the lining. However, these benefits are not used in a standard linear-elastic structural analysis. The structural and economic potential can be activated in an in-elastic structural analysis using, for example, a concept typically used for a simplified method for an in-elastic design of steel frames.

Structurally a cracked FRC lining acts like a “plastic hinge,” which still transfers a moment while rotating. In a classical elastic analysis, the capacity of the plastic hinges could be used as follows for a quasi inelastic procedure: While increasing the load on a tunnel lining, the peak elastic moment will be reached at a specific point. The elasto-plastic or strain-hardening behavior would allow for the introduction of a hinge at this location and altering the overall static (elastic) system of the lining. In a next step, the external

load would be increased further until the peak elastic moment would be reached at another location and another hinge would be introduced at this location, and so forth.

At the end of this process, the moments of each step would be superimposed and added. While increasing the external loads during this process, the values of the moments at the hinges could not be increased beyond the plastic moment, but the rotation could increase, making the overall system “softer.” Following this approach, the lining would be locally weakened to induce a load redistribution and eventually show a system failure rather than failure at a specific cross section. The ultimate stage would be reached either as a result of system failure or by reaching rotation thresholds at the hinges or some other predefined limits. Given the properties of a tunnel lining as an embedded beam, a system failure would basically mean formation of hinge next to hinge in close proximity. For this reason, other meaningful structural thresholds or definition of a maximum number of hinges seem to be a viable option. The procedure described previously would allow full use of the properties and benefits of FRC in a structural analysis, while still using elastic structural analysis tools.

CONCLUSIONS

The article has presented and discussed the basics of FRC tunnel lining design using a selected SSR. The impact of normal force within the tunnel lining and the impact of a change of post-cracking behavior from strain softening to strain hardening was discussed in detail by means of a parametric study.

Current tunnel lining design does not fully use the potential of FRC because it disregards the positive benefits of the compressive force, which are not related to the material properties itself. Future material specifications for tunnels should consider the expected range of compressive stress in the lining and its beneficial influence on the ductility of FRC. The most advantageous property of FRC is its toughness when the tunnel lining has cracked. The potential of the toughness is currently not typically used when evaluating moment resistance in the cracked state under a simultaneous axial force. A procedure to introduce plastic hinges has been suggested that would allow use of the benefits of FRC using classical structural analysis tools and thereby realize the full structural and economic potential of FRC.

References

1. ACI Committee 544, “Report on Indirect Methods to Obtain Stress-Strain Response of Fiber-Reinforced Concrete (FRC) (ACI 544.8R-16),” American Concrete Institute, Farmington Hills, MI, 2016, 22 pp.
2. ACI Committee 544, “Design Considerations for Steel Fiber Reinforced Concrete (ACI 544.4R-88) (Reapproved 2009),” American Concrete Institute, Farmington Hills, MI, 1988, 18 pp.
3. ACI Committee 544, “Report on Design and Construction of Fiber-Reinforced Precast Concrete Tunnel Segments (ACI 544.7R-16),” American Concrete Institute, Farmington Hills, MI, 2016, 36 pp.
4. ACI Committee 506, “Guide to Fiber-Reinforced Shotcrete (ACI 506.1R-08),” American Concrete Institute, Farmington Hills, MI, 2008, 12 pp.

5. German Society for Concrete and Construction Technology (DBV), “Guide to Good Practice – Steel Fibre Concrete,” 2001.
6. Deutscher Ausschuss fuer Stahlbeton (German Committee for Reinforced Concrete) (DAfStb), DAfStb Richtlinie fuer Stahlfaserbeton (DAfStb Guideline for Steel Fiber Reinforced Concrete), 2010. (in German)
7. Barton, N.; Lien, R.; and Lunde, J., “Engineering Classification of Rock Masses for the Design of Tunnel Support,” *Rock Mechanics*, V. 6, No. 4, 1974.
8. Grimstad, E., and Barton, N., “Updating of the Q-System for NMT. In Kompen,” Opsahl & Berg (eds), *Proceedings of the International Symposium on Sprayed Concrete—Modern Use of Wet Mix Sprayed Concrete for Underground Support*, Fagernes, Norway, 1993.
9. Nitschke, A., “Tragverhalten von Stahlfaserbeton für den Tunnelbau (Load Bearing Behavior of Steel Fiber Reinforced Concrete for Tunneling),” PhD thesis, Technisch-wissenschaftliche Mitteilungen des Instituts für konstruktiven Ingenieurbau der Ruhr-Universität Bochum, TW 98-5, 1998. (in German)
10. Dietrich, Jörg, “Zur Qualitätsprüfung von Stahlfaserbeton für Tunnelschalen mit Biegezugbeanspruchung (About Quality Testing of Steel Fiber Reinforced Concrete for Tunnel Lining under Flexural Tension),” PhD thesis, Technisch-wissenschaftliche Mitteilungen des Instituts für konstruktiven Ingenieurbau der Ruhr-Universität Bochum, TW 92-4, 1992. (in German)
11. ACI Committee 318, “Building Code Requirements for Structural Concrete (ACI 318-14) and Commentary (ACI 318R-14),” American Concrete Institute, Farmington Hills, MI, 2014, 519 pp.
12. ACI SP-17(14), *The Reinforced Concrete Design Handbook, Volume 1: Member Design*, American Concrete Institute, Farmington Hills, MI, 2015.
13. Maidl, B., *Steel Fibre Reinforced Concrete*, Ernst & Sohn, Berlin, Germany, 1995.
14. Nitschke, A., and Ortu, M., “Bemessung von Stahlfaserbeton im Tunnelbau. Abschlußbericht. (Design of Steel Fiber Reinforced Concrete for Tunneling. Final Report),” Ruhr-Universität Bochum, Lehrstuhl Prof. Maidl, Research Project funded by the Deutscher Beton-Verein E.V. (DBV-Nr. 211) and the Arbeitsgemeinschaft industrieller Forschungsvereinigungen (AiF-Nr. 11427 N), Fraunhofer IRB Verlag, 1999. (in German)
15. Maidl, B.; Nitschke, A.; and Ortu, M., Bemessung von Tunnelschalen mit dem M/N-Prüfkonzept. (Design of Tunnel Linings with the M/N Testing Concept), Taschenbuch für den Tunnelbau 1999, Glückauf Verlag, Essen, 1998.



Axel G. Nitschke is Vice President of Shannon & Wilson Inc. He received his MSc and PhD in civil engineering from Ruhr University Bochum, Bochum, Germany, in 1993 and 1998, respectively. He has gained more than 20 years of in-depth, on-the-job experience in all aspects of underground construction, geotechnical engineering, and mining. He has worked on the engineering and construction of many tunnel projects in Europe, the United States, Canada, and Colombia. He is well-experienced in all ground conditions, ranging from soft ground to hard rock, and the associated implications for design and construction methods. Nitschke has held key positions, such as Senior NATM Engineer, Contract/Claims Manager, Risk Manager, Design Manager, and Project Manager. He currently serves on the ASA Board of Direction and Chairs the ASA Underground Committee. He is a licensed professional engineer in Virginia, Maryland, the District of Columbia, New Jersey, Washington, and California.